

Evaluation for Small Visual Difference Between Conforming Meshes on Strain Field

Zhe Bian¹ (边 哲), Shi-Min Hu¹ (胡事民), and Ralph R. Martin²

¹*Department of Computer Science and Technology, Tsinghua University, Beijing 100084, China*

²*School of Computer Science, Cardiff University, Cardiff, U.K.*

E-mail: bz05@mails.tsinghua.edu.cn; shimin@tsinghua.edu.cn; Ralph.Martin@cs.cardiff.ac.uk

Received June 4, 2008; revised December 1, 2008.

Abstract This paper gives a method of quantifying small visual differences between 3D mesh models with conforming topology, based on the theory of strain fields. Strain field is a geometric quantity in elasticity which is used to describe the deformation of elastomer. In this paper we consider the 3D models as objects with elasticity. The further demonstrations are provided: the first is intended to give the reader a visual impression of how our measure works in practice; and the second is to give readers a visual impression of how our measure works in evaluating filter algorithms. Our experiments show that our difference estimates are well correlated with human perception of differences. This work has applications in the evaluation of 3D mesh watermarking, 3D mesh compression reconstruction, and 3D mesh filtering.

Keywords 3D conforming meshes, mesh comparison, perception, strain fields

1 Introduction

3D surface triangle meshes are widely used in computer graphics and modelling; techniques such as watermarking, filtering and compression are often applied to meshes.

Watermarking is used to hide an “invisible” digital signature into the mesh for information security and digital rights management^[1–6]. The watermark information is encoded into small perturbations to the model’s description, e.g., its vertex coordinates, changing the model’s geometry by a small amount. Little work has been done on methods of evaluating the *quality* of watermarking schemes, which involves the *perceptibility* of the watermark (and other considerations such as how difficult it is to remove the watermark, etc.). Mesh models constructed from 3D scanner data must be *denoised* before they are suitable for application purposes^[7]. More generally, various *filters* may be applied to meshes to modify them in some way^[8]. It is useful to be able to assess the *visual impact* of filtering algorithms. Both to economize the use of bandwidth, and to saving storage, *mesh compression* are useful^[9–12]. Evaluation of *visual differences* between the reconstructed version and the original are again important.

Here, we give a new method of quantifying small visual differences between conforming meshes (i.e., meshes with the same number of triangles, connected in the same way). Conforming modification is often made in watermarking and filtering schemes, but perhaps less so in other applications. And such a quality measure should agree with human perception, which is subjective and hard to quantify^[13]. Nevertheless, our methodology, based on strain fields, provides a measure which is well correlated with perceptual results provided by human subjects.

The rest of this paper is organized as follows. Section 2 describes the related work. Section 3 explains strain fields, and shows how to compute strain in a mesh. Section 4 discusses how to compute a perceptibility distance based on strain energy. Section 5 and Section 6 describe an experiment recording human perception of visual changes in meshes, and experimental tests of our proposed methodology, including comparisons with other filter approaches. Conclusions are drawn in Section 7.

2 Related Work

If a watermark becomes too obvious, distorting the model too much, the watermarking scheme is

Regular Paper

This work was supported by the National Basic Research 973 Program of China under Grant No. 2006CB303104, the National Natural Science Foundation of China under Grant No. 60673004, and an EPSRC Travel Grant.

The preliminary version of this paper and the early version for this work has been published on GMP2008.

unacceptable. We may also wish to *compare* the perceptibility of the same watermarking information added by different schemes when deciding which scheme to adopt. A method adapted from image watermarking assessment is given by [14], while [15] provides two methods based on surface roughness. Few objective methodologies have been proposed, and even less attention has been paid to subjective evaluation^[16]. As static 2D images of 3D models are inadequate for assessing the quality of a 3D model, there is a need for 3D quality metrics.

Other papers have discussed evaluation of the visual effects of mesh compression and filtering. Some are based on perceptual metrics taken from image processing^[14], others consider geometric differences^[15,17,18], and yet others combine both^[19]. However, assessing perceptual degradation of images and 3D models are different tasks. [17, 18] only consider geometric errors based on Hausdorff distance, which do not correlate well with human perception^[15]. The two methodologies in [15] are better. One measures mesh distortion using roughness based on dihedral angles between faces. The other uses an equation based on variance of displacements (between the original and the smoothed meshes) along the normals of vertices in a 2-ring area of each vertex with its performance depended on smooth algorithms. One limitation is that these metrics use the roughness of the original mesh for normalization. If the roughness is large, distortion of smooth parts of the mesh is not captured, yet may be quite visible to an observer. These methods also take time more than linear because of the number of mesh faces.

The most direct way of evaluating perceptibility of a change in a 3D mesh is to ask human observers. However, using enough “typical” (whatever that means) human observers is time consuming and costly. Human beings do not give consistent and repeatable answers. Such tests can easily introduce bias. Thus, objective methodologies are preferable for assessing visual changes in meshes. This paper provides such a methodology, producing results well-correlated with those from human observers, in our limited testing. Our approach analyzes shape and size changes of mesh triangles, ignoring any rigid-body motion. We use *strain energy* to quantify the deformation.

3 Strain Fields

3.1 Basic Principle

Strain and *stress* are used to describe pointwise mechanical behaviour inside a solid body^[20]. At any

point, strain represents the local deformation and the local force respectively. Isotropic linear elasticity is the simplest mathematical model for continuum mechanics. And from [20] we know that the strain applied to mesh models is reasonable.

The effects of the mesh processing algorithm under evaluation can be seen as equivalent to applying a fictitious external force which distorts the 3D mesh. We use the idea of *strain field* to analyze the deformation of the mesh. Changes in position of the mesh vertices represent distortion of the mesh, but also incorporate a rigid-body motion which leaves the shape unchanged. To remove this rigid body motion, we use the concept of *strain*.

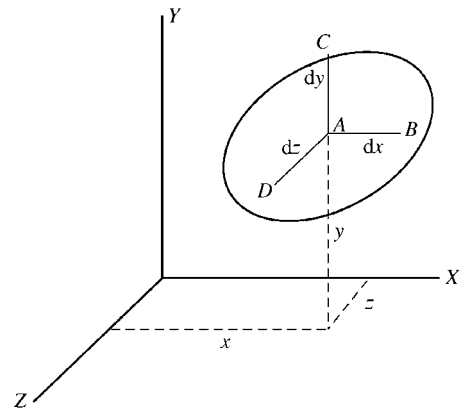


Fig.1. Local deformation within an object.

In Fig.1, let A be some arbitrary point of the object. Consider three infinitesimal segments AB , AC , and AD , parallel to the coordinate axes and with lengths dx , dy and dz . When the object is acted upon by an external force, both the *lengths* of these lines and the *angles* between them change. The fractional changes in the lengths are called the *normal strain* at A , denoted by ϵ_x , ϵ_y and ϵ_z , respectively. The fractional changes in the angles are called the *shear strain*, denoted by γ_{xy} , γ_{yz} and γ_{zx} , respectively. If the local deformation and rotation are small, the relation between strain and displacement is linear^[20]:

$$\begin{aligned}\epsilon_x &= \partial u / \partial x, & \gamma_{xy} &= \partial v / \partial x + \partial u / \partial y; \\ \epsilon_y &= \partial v / \partial y, & \gamma_{yz} &= \partial w / \partial y + \partial v / \partial z; \\ \epsilon_z &= \partial w / \partial z, & \gamma_{zx} &= \partial u / \partial z + \partial w / \partial x.\end{aligned}\quad (1)$$

Deformation of a solid body requires *strain energy*. Associated with the local deformation, described by strain, there is a local force, *stress*, distributed throughout the object. The stress on some point is the limit of the local force acting on a differential area around the point, which can be decomposed into two parts: the normal stress σ perpendicular to the surface and the

shear stress τ within the surface^[21]. The strain energy is the work done by the stress on the corresponding strain.

3.2 Strain in a Mesh

We now discuss how strain and stress can be used to provide a measure of perceptibility of differences between two conforming meshes.

A 3D mesh is a shell composed of triangular faces of negligible thickness. If the mesh is distorted slightly, and we assume that its faces do not bend, to a first approximation the mesh triangles are unchanged in their normal direction: only their shapes and positions change^[22]. Any elastic deformation only occurs within the plane of each triangle, see Fig.2. The strain for each triangle can thus be computed in its own plane by ignoring any rigid body motion. So we can interpolate the vertices displacement functions of deformation across each triangle, and compute the strain for each triangle.

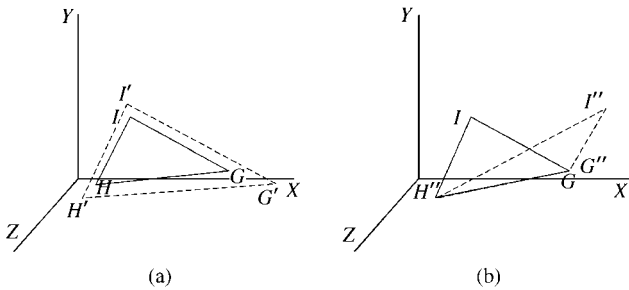


Fig.2. Area and distortion deformation. (a) Area deformation. (b) Distortion deformation.

As we assume that each triangle deforms entirely within its own plane, there is no deformation or strain normal to each triangle. Thus, following the approach in [22], (1) may be simplified in this case:

$$\begin{aligned} \epsilon_x &= \frac{\partial u}{\partial x}, & \epsilon_y &= \frac{\partial v}{\partial y}, & \epsilon_z &= \frac{\nu}{\nu-1}(\epsilon_x + \epsilon_y), \\ \gamma_{xy} &= \frac{\partial v}{\partial x} + \frac{\partial u}{\partial y}, & \gamma_{yz} &= 0, & \gamma_{zx} &= 0, \end{aligned} \quad (2)$$

where ν is Poisson's ratio (see later). We can now compute ϵ_x , ϵ_y and γ_{xy} from the displacement functions u , v obtained above.

3.3 Strain Energy

As strain field has different physical meanings and different directionalities, it is not easy to construct a composite measure on them. The key is to use the concept of *strain energy*. Using the relations between stress and strain, the *strain energy* may be written as tensor

form^[20]:

$$W = \frac{1}{2} \left(\left(\lambda + \frac{2}{3}G \right) \epsilon_{ii}^2 + (2G) \epsilon'_{ij} \epsilon'_{ij} \right) S_{\Delta}, \quad (3)$$

where S_{Δ} is the area of each triangle, and E is *Young's modulus*, ν is *Poisson's ratio*, $\lambda = E\nu/((1+\nu)(1-2\nu))$ is *Lamé's first parameter*, and $G = E/(2(1+\nu))$ is the *shear modulus*: these physical quantities determine the material's elastic properties. We simply fix them in our methodology to $E = 1$ and $\nu = 0$. And we can adjust them to improve the result according to subjective experiments, but in our experiments these choices give good results.

4 Perceptibility

Following an approach used for images^[3], we define a *perceptual distance* $P(m_0, m_p)$ between the original model m_0 and the processed model m_p : the larger the perceptual distance, the more visible the difference between them. Our experiments show that we can define such a function using strain energy which agrees well with human perception. We first consider two special situations of strain energy in meshes, then give the final perceptible function.

4.1 Improvements

Distortions in 3D meshes may be of varying kinds, with varying perceptibilities. And there are some situations which are not described well by strain energy. We therefore considered how we might improve upon the basic ideas above. In particular, we considered two ideas projection and edge triangles.

Projection. Many applications of 3D meshes render them. The most important quantity determining the appearance of a triangle is its normal vector. Strain energy does not directly capture this idea. For example, when vertices are displaced within the local tangent plane of the mesh, the strain field can be large although a rendered image remains almost the same. Consider several adjacent triangles which lie in the same plane, and hence have the same normals. We may consider two types of distortions involving these triangles: the one in which the center vertex still lies in the plane, and the one in which the center vertex moves perpendicularly to the tangent plane. The former distortion has no visual effect, and thus should be ignored. More generally, we can represent any local distortion as a combination of within-tangent-plane distortion and normal distortion. To remove the contribution of the in-tangent-plane distortion, we project the vertex, after distortion, back into the original tangent plane, and calculate the strain

energy with respect to this adjusted position of this common vertex.

Edge Triangles. Triangles in different locations generally have differing visual impact. For a model with smooth faces bounded by sharp edges, distortions in triangles at edges are likely to be more noticeable. We thus accordingly apply a weight w_i to each triangle's strain as follows. We set $w_i = \pi - \alpha_i$, if α_i is less than $\pi/2$, and $w_i = 1$ otherwise, where α_i is the smallest dihedral angle between face i and its neighbours.

As we will see later, these two proposed improvements actually have little useful effect on our results.

4.2 Perceptual Distance

We now consider how to convert strain energy into a *perceptual distance*. The distortion must be measured based on *relative* to the size of the model, and should also be independent of the number of triangles. We thus define the *perceptual distance* $P(m_o, m_p)$ as the weighted average strain energy (ASE) over all triangles (processing tangent triangular faces), and normalized by S , the total area of the triangular faces:

$$P(m_o, m_p) = \frac{1}{S} \sum w_i W_i. \quad (4)$$

5 Evaluation

We now give three experiments, and show that our measure of perceptibility produces results that correlate well with those assessed by human subjects.

Experiment I gives human opinions concerning the perceptibility of changes caused by making changes to models used in Experiments II and III. Experiment II considers two simple measures of perceptibility of changes, based on triangle areas, and triangle normals, and shows that we do better than use such simple measures. Experiment III tests the candidate improvements.

5.1 Experiment I: Human Perception of Differences Versus Strain Field Measure

To obtain some ground truth, i.e., subjective human results of the perceptibility of various changes in mesh models is needed^[13], we followed the approach in [15]. We embedded data into mesh models of a chess king and a horse, using the *Triangle Similarity Quadruple* (TSQ) watermarking method in [5], and a noise embedding method.

To measure the subjective degree of mesh deformation perceived by human observers, we produced

meshes with different amounts of deformation. We prepared variants of the horse, and of the chess king, resulting in 15 meshes for each: the undeformed model, 7 with watermarks embedded in different parts of the mesh, incorporating different amounts of data, and 7 with different amounts of noise embedded at different places. It is easy to find the differences of these models from the original and also easy to tell apart each other. Subjects were asked to rate the differences between the original and processed models on a scale from 0 to 10, where 0 meant identical and 10 meant very dissimilar, to give an *opinion score* (OS).

In order to help the subjects evaluate differences in the 3D mesh models, we paid careful attention to the rendering conditions, as suggested in [15]:

- *Color.* We used black for the background to help models stand out. Models were coloured grey, which makes edges more visible and deformations easier to see.

- *Light Source.* All models used the same single white point light source, because multiple lights can confuse observers.

- *Lighting.* Although a local illumination model can produce more realistic effects for textured models, it can hide the parts with high distortion. Thus we used a global illumination model. We also set diffused and specular reflections to models for reality.

- *Texture.* Models were untextured, as textures can hide any distortion.

- *Test Subjects.* 30 test subjects (20 male, 10 female) were drawn from a pool of computer science students aged 22~25. For impartiality, some of the chosen test subjects had knowledge of computer graphics, and others did not.

- *Screen and Model Resolution.* The models were displayed on a 17-inch LCD monitor, with resolution 1280×1024 . The watermarked and original models were displayed together so as to fill the screen. The chess king model had 12170 triangles and horse model had 10024 triangles, allowing clear observation of detail. The screen was viewed from a distance of approximately 0.6m.

- *Interaction.* We allowed the subjects to rotate and zoom the models. [16] suggests that evaluation of alterations to 3D objects should permit interaction.

The experiment comprised three steps:

- 1) *Oral Instructions and Training.* First, we told the subjects about 3D mesh models, watermarking, compression and filters. We then gave examples of an unaltered mesh, to be scored as 0, and a worst-case altered mesh, to be scored as 10.

- 2) *Practice with a Sample Model.* Next, the subjects were allowed to interact with various processed models

to familiarize themselves with the experiment.

3) *Experimental Trials.* In this step, the subjects were asked to score the differences between the original models and altered models.

While human observers were rather variable in their opinions as to perceptibility of differences, there was general correlation between average strain energy (ASE) and opinion scores, as will be discussed in more detail in the next section. Figs. 3(a) and 3(b) show plots of the individual opinion scores (OS) against strain energy. Each circle in Fig.3(a) and cross in Fig.3(b) correspond to one model assessed by one subject.

In subsequent experiments, we used the *means* of these human opinion scores (MOS) for each altered model as being representative of the amount of visual differences perceived by human subjects.

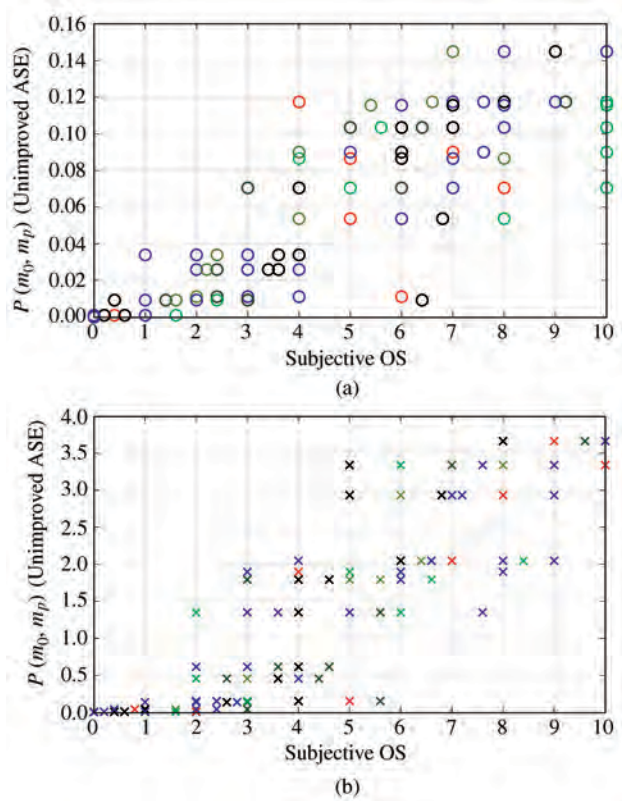


Fig.3. Unimproved ASE perceptual distance versus subjective opinion score (OS). (a) Horse. (b) Chess king.

5.2 Experiment II: Strain Field Measure Versus Other Simpler Measures

We next investigated the relationship between mean opinion score values (MOS) and two other simple perceptual distance measures which might plausibly be used for assessing mesh distortion: the *fractional*

change in the total area of the triangles (P_{FTAR}) and the *fractional change in angle between normal vectors of adjacent faces* (P_{FNVANG}). The first of these measures is defined as follows:

$$P_{\text{FTAR}}(m_0, m_p) = \frac{\sum_{i=1}^n |\Delta S_i|}{\sum_{i=1}^n S_i},$$

where n is the number of faces of the mesh, ΔS_i is the change in area of face i and S_i is its area. The second is defined as

$$P_{\text{FNVANG}}(m_0, m_p) = \frac{\sum_{i=1}^m |\Delta \alpha_i|}{\sum_{i=1}^m \alpha_i},$$

where m is the number of the edges of the mesh, $\Delta \alpha_i$ is the change in angle of normal vectors between edge i , and α_i is the angle of normal vectors between edge i .

Initially, we used three methodologies, unimproved ASE, FTAR and FNVANG, to separately evaluate the effects of watermarking and noise addition with different amounts of added information or noise. Fig.4 shows that *all* evaluation methodologies give results well correlated with the mean opinion scores from Experiment

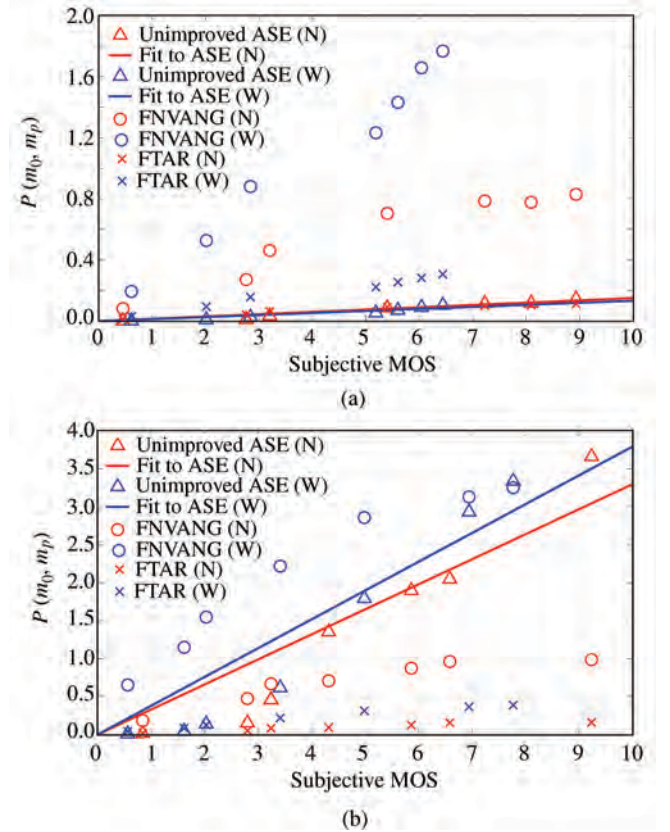


Fig.4. Various perceptual difference measures versus mean subjective opinion score (MOS) done with watermarking and noisy separately (watermarking is noted by W and noisy is noted by N). (a) Horse. (b) Chess king.

I. Table 1 shows the corresponding correlation coefficients. It is perhaps unsurprising that each assessment methodology gives a consistent result when the *same* processing method is used to distort the mesh more and more.

Table 1. Correlation Between Various Perceptual Distance Measures and Human Opinion Done With Watermarking and Noisy Separately

Perceptual Distance Based on	Correlation Coefficient	
	Horse	Chess King
FTAR (W)	0.9925	0.9854
FNVANG (W)	0.9893	0.9699
<i>unimproved</i> ASE (W)	0.9669	0.9827
FTAR (N)	0.9710	0.9552
FNVANG (N)	0.9622	0.9282
<i>unimproved</i> ASE (N)	0.9814	0.9776

Note: W — watermarking, N — noisy

However, a good evaluation method should be independent of the way in which the mesh has been distorted. We thus put the distorted meshes produced by watermarking and adding noise into a single set, and did the experiment again. Fig.5 shows that the mean opinion scores from Experiment I are now *not* well

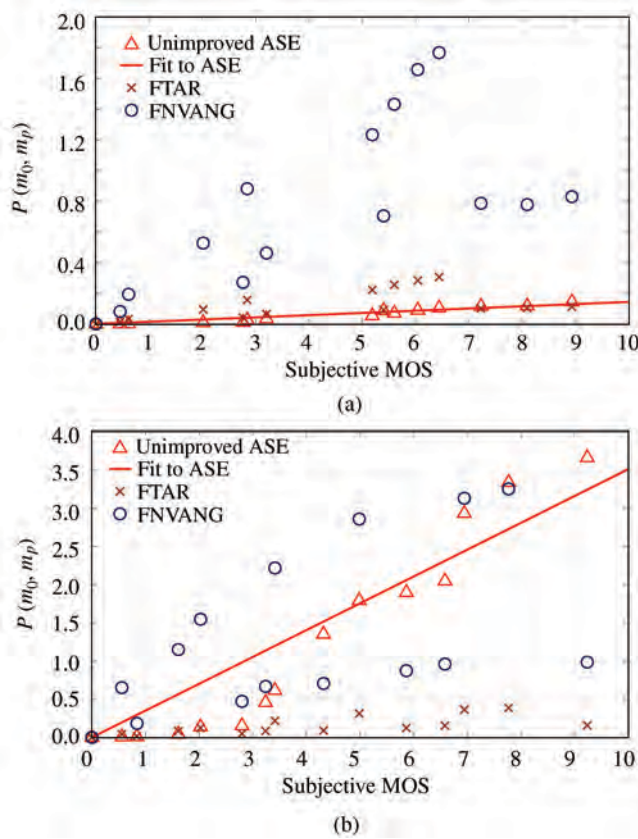


Fig.5. Various perceptual difference measures versus mean subjective opinion score (MOS). (a) Horse. (b) Chess king.

correlated with the proposed P_{FTAR} or P_{FNVANG} perceptual distances, either for the horse or the chess king — we can see these two simpler perceptual distance measures produce much more scattered results than the average strain energy measure. They do not adequately predict human opinion of mesh differences — whereas the strain field perceptual distance measure produces results which lie much closer to a straight line.

To more precisely analyze this observation, we calculated the correlation coefficient between each perceptual distance measure and the human mean observation scores, see Table 2. The simpler FTAR and FNVANG perceptual distances have much lower correlation than our *unimproved* ASE strain energy perceptual distance, and hence are of less value for measuring human opinion of distortion. We further conclude that, given the very high correlation coefficients observed, the (unimproved) perceptual distance based on strain energy is a useful replacement for subjective mean human opinions of mesh differences.

Table 2. Correlation Between Various Perceptual Distance Measures and Human Opinion

Perceptual Distance Based on	Correlation Coefficient	
	Horse	Chess King
FTAR	0.56	0.71
FNVANG	0.67	0.54
<i>Unimproved</i> ASE	0.97	0.97

From a mathematical point of view, we believe the better performance of the ASE perceptual distance arises because strain energy provides a well-defined L^2 measure in deformation space, unlike FTAR and FNVANG.

5.3 Experiment III: Variants of Strain Energy Measure

We next investigated the relationship between strain energy and mean opinion score values (MOS) when using the suggested improvements based on projection and edge weights (see Subsection 4.1). We compared 4 variants of our method: *unimproved* perceptual distance (without projection and face weights), perceptual distance using projection, perceptual distance using edge weights, and perceptual distances using both projection and edge weights.

Fig.6 shows a comparison of these four different measures with mean human opinion scores, as in Experiment II. In each case a similar close-to-linear relationship can be seen in both horse and chess king models. Using the projection idea has almost no effect on perceptual distances. Using edge weighting has a bigger effect (see Fig.6), although there is no obvious

improvement in terms of linearity of relationship. The probable reason is that the models used (like many models) have relatively few flat regions or sharp triangles. We also note that the subjective scores are not very exact, making it difficult to distinguish whether the results before and after these modifications are really an improvement. Again correlation coefficients were computed and are given in Table 3. The edge weights *do* make a small improvement in the horse model, but have the opposite effect on projection, while for the chess king model, the opposite is true, projection making a small improvement but edge weighting being worse. Ultimately, our experiments show no benefit of using either suggested improvement: there is almost no difference in correlation between the computed measure

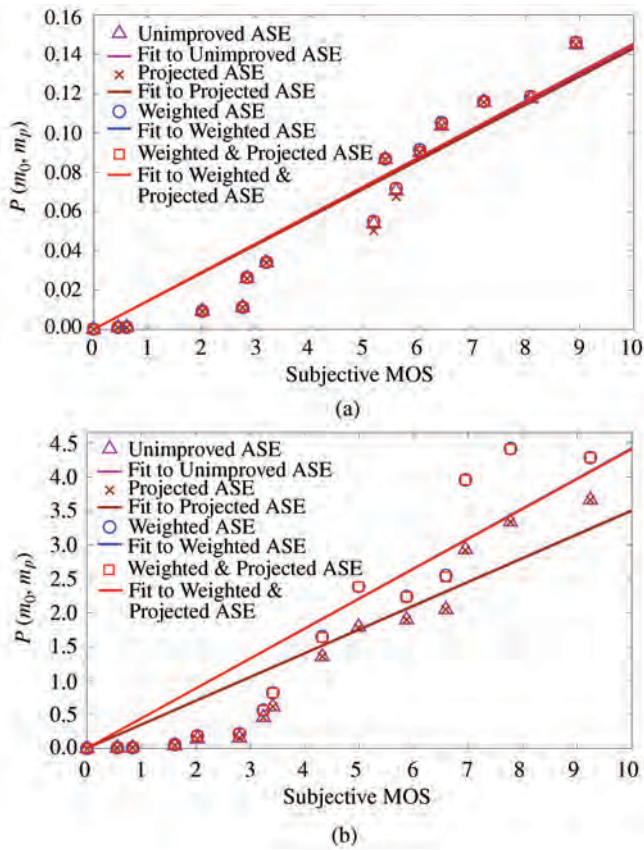


Fig.6. Kinds of ASE perceptual distance and mean subjective opinion score (MOS). (a) Horse. (b) Chess King.

Table 3. Correlation Between the Four Perceptual Distance Measures and Human Opinion

Perceptual Distance Based on	Correlation Coefficient	
	Horse	Chess King
<i>unimproved</i> ASE	0.9745	0.9660
<i>projected</i> ASE	0.9715	0.9661
<i>weighted</i> ASE	0.9751	0.9560
<i>projected & weighted</i> ASE	0.9752	0.9557

and human. We thus recommend the use of the *unimproved* opinion. ASE-based perceptual distance, as it is simpler to compute. The other methods increase the computation time, without noticeable benefit.

5.4 Analysis

In this subsection, we analyze the experiments we have done to discuss relation between visual perception and our method.

From Experiment II, we can see that when we evaluate the effects of watermarking and noise addition our method does not have any superior performance. But the visual perception is very close to the degree of local deformations and the area of deformation: when some location is distorted more, people will find the difference more easily; when the deformation area is larger, people can also find the difference but not so easily as the former. The strain energy considers both situations: it will increase faster when the local deformations on elastic body become bigger and also increase fast when the area of deformation is enlarged. From Table 1 we can see that our method gives better results of noise processing than that of watermarking because strain field pays more attention to the local deformation. And in the experiment evaluating the two processed methods together, we can see our method is accordant to subjective judgment. Experiment III gives us a result that our improvement is less active, the probable reason is the limitation of our experimental models: they both have few sharp edges. But to observe readily the difference in Experiment I, we have to select the flat models.

Ultimately, the number and type of subjects used in these experiments were limited, as were the number and types of test models, and the range of methods used to add distortion to the models. We acknowledge that considerable further testing is necessary for fully validating these conclusions.

6 Further Demonstrations

We now provide two further demonstrations of our approach. The first is intended to give the readers a visual impression of how our measure works in practice, while the second demonstrates an application of our methodology.

6.1 Demonstration I: Distortion in a Buddha Model

Here we simply present a series of Buddha models, with 62 224 faces, which have been processed by watermarking (Figs. 7(a)~7(f)) and noise addition (Figs. 7(g)~7(l)) algorithms, making changes controlled by

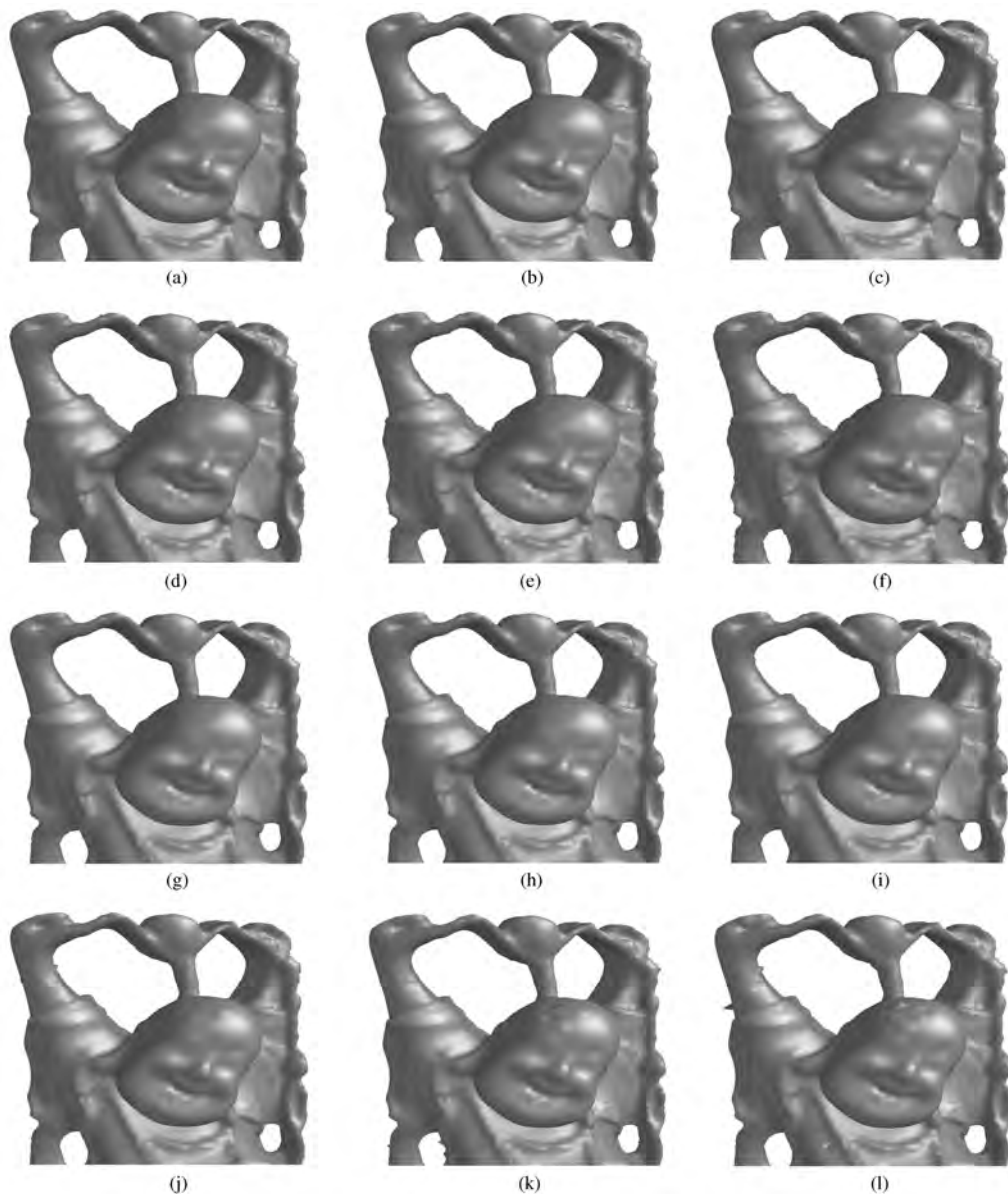


Fig.7. (a)~(f) Watermarked Buddhas. (g)~(l) Buddhas with added noise.

Table 4. Perceptual Distance Based on Strain Energy $P \times 10^{-5}$ for Buddhas with Varying Deformations

Watermarked Models	FTAR	P	Models with Noise	FTAR	P
(a)	0	0	(g)	0	0
(b)	661	4	(h)	115	4
(c)	3 335	114	(i)	568	114
(d)	6 644	455	(j)	1 074	523
(e)	10 020	1 042	(k)	1 702	1 778
(f)	12 342	1 533	(l)	2 313	3 988

successively increasing the FTAR measure as stated in Table 4, which also gives the perceptual distances of these models from the unperturbed model. These figures and numbers allow the readers to gain some

impression of their own concerning our (unimproved) perceptual distance measure.

6.2 Demonstration II: Application to Comparison of Mesh Filter Methods

We now provide further the other demonstration which gives readers a visual impression of how our measure works in evaluating filter algorithms. Here we only use unimproved evaluating method for demonstration. The two filter algorithms used for comparison are Laplacian filter^[8] and Gaussian filter^[23]. First we only filter the original model using two pendent filter algorithm with different times to show their effects, and

then filter the noisy model to compare which filter algorithm is better. The model we used is horse model with 10 024 faces, see Fig.8(a), which is smooth enough to show the visual differences. The meshes were distorted by Gaussian noise with the order of magnitude 0.1. In this demonstration we set the damping factor λ as 0.6 for Laplacian filtering^[8], while the σ_f as 0.7 in spatial weight function and the σ_g as 0.3 in influence weight function for the Gaussian filtering^[23].

From [8] we know that if the models are filtered more over by Laplacian filter they will shrink obviously, while the Gaussian filter in [23] is better at keeping original features. This will be demonstrated as follows. In Fig.9, we can see a series of results gotten by Laplacian and Gaussian filters: when horse is filtered once by Laplacian filter, the feature will be kept well; if more, it will shrink more acutely. But the feature is always kept well regardless of filter time by Gaussian filter. The same result is shown in Table 5.

Then we added Gaussian noise to horse model and filtered it with these two filter algorithms. The noisy

model is shown in Fig.8(b), and the strain energy between original and noisy models is 1.974 25 which is big enough to show the effects of the two introductive filter algorithms. We show the filter results in Fig.10. When filtering the noisy model once or 3 times, the results are little different. Both Laplacian filter and Gaussian filter have their advantages and disadvantages. The Laplacian filter smoothed most of noise but also smoothed

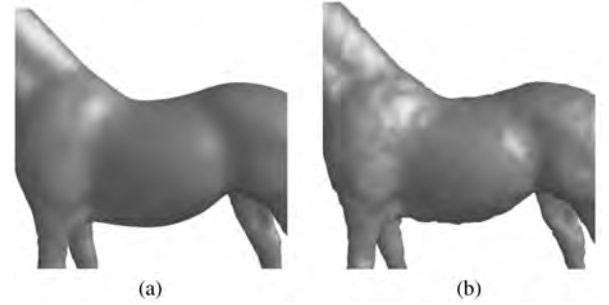


Fig.8. Original and noisy models of horse. (a) Original model. (b) Noisy model.

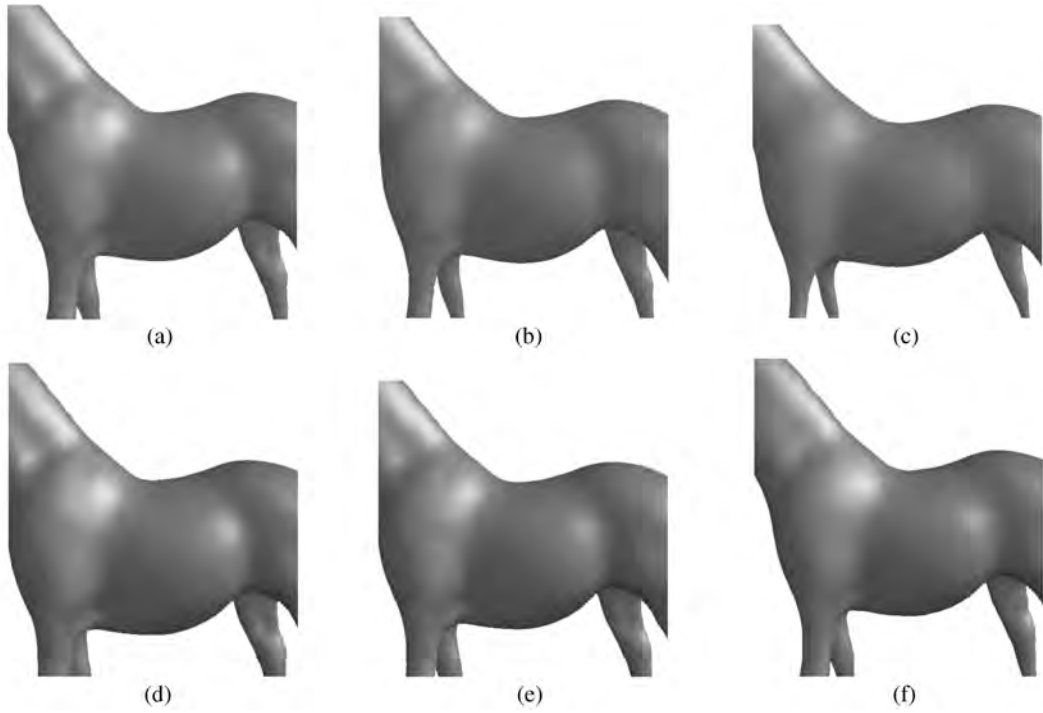


Fig.9. Filtering original models. (a) Filtering once by Laplacian filter. (b) Filtering 3 times by Laplacian filter. (c) Filtering 10 times by Laplacian filter. (d) Filtering once by Gaussian filter. (e) Filtering 3 times by Gaussian filter. (f) Filtering 10 times by Gaussian filter.

Table 5. Perceptual Distance Based on Strain Energy $P \times 10^{-5}$ for Horse with Varying Filters

Laplacian Filter	P	Gaussian Filter	P	Laplacian Filter	P	Gaussian Filter	P
Fig.9(a)	14 360	Fig.9(d)	12 714	Fig.10(a)	14 201	Fig.10(d)	14 194
Fig.9(b)	16 874	Fig.9(e)	12 907	Fig.10(b)	16 445	Fig.10(e)	14 406
Fig.9(c)	22 903	Fig.9(f)	13 314	Fig.10(c)	23 078	Fig.10(f)	14 955

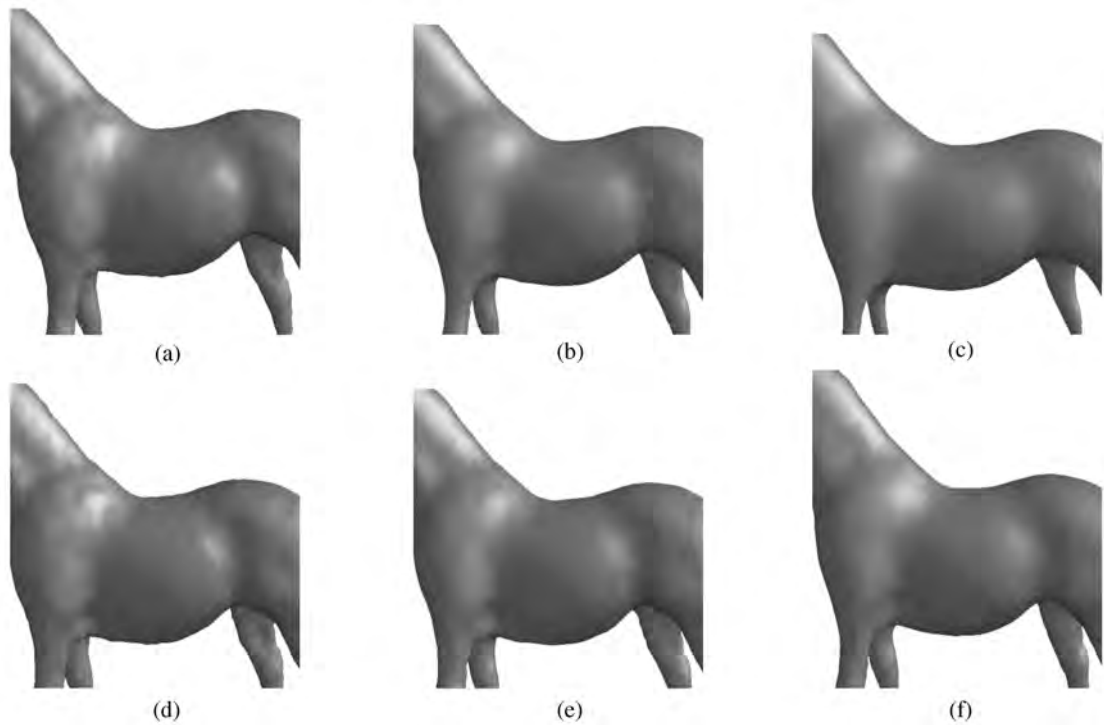


Fig.10. Filtering noisy models. (a) Filtering once by Laplacian filter. (b) Filtering 3 times by Laplacian filter. (c) Filtering 10 times by Laplacian filter. (d) Filtering once by Gaussian filter. (e) Filtering 3 times by Gaussian filter. (f) Filtering 10 times by Gaussian filter.

small-scale features, while the Gaussian filter kept features well but still kept some largish-scale noise at the same time. When we increased the filtering time (e.g., 10 times), the model filtered by Laplacian filter shrank much obviously while the large-scale features still were kept well enough by Gaussian filter. Table 5 gives the conclusion.

7 Conclusions and Future Work

This paper has proposed a new methodology for comparing small visual differences between conforming models. Our methodology is based on the use of strain field theory to quantify deformation produced by some process. Our experiments show that this objective method can produce results which are strongly correlated with the average of subjective human opinions. The same is *not* true of simpler measures based on changes in triangle areas, or surface normals.

This work has applications to assessing the perceptible effects of 3D mesh processing algorithms such as watermarking, compression and other filtering. For example, in watermarking we could use this approach to

decide which part of a model is the most suitable place for embedding a watermark and how much data can be hidden in a mesh model, or to choose between watermarking schemes.

Our methodology has certain limitations. One is that for certain objects, such as engineering components, sharp edges are very important, yet involve few triangles. The second is that the method is based on deformation of the triangular faces, yet a model may in principle deform without changes in the size and shape of faces. We assume that the strain in a mesh model occurs only in the surface of the model. Hence, the associated strain energy only measures intrinsic deformation in the surface, and deformation in the normal direction is ignored. Our experiments also clearly have some limitations. Ideally, the numbers and types of persons, models, and processing algorithms used in evaluation would be much higher.

One area we wish to explore in future is to try to statistically determine thresholds of perceptibility through subjective experiments, which can then be used with our method to decide whether a visual difference is perceptible.

References

- [1] Agarwal P, Adi K, Prabhakaran B. Robust blind watermarking mechanism for motion data streams. In *Proc. 8th Workshop on Multimedia and Security*, Geneva, Switzerland, Sept. 2006, pp.230–235.
- [2] Arnold M, Wolthusen D, Schmucker M. Techniques and Applications of Digital Watermarking and Content Protection. Artech House Publishers, 2003.
- [3] Cox I, Miller M, Bloom J, Miller M. Digital Watermarking: Principles & Practice. Morgan Kaufman, 2002.
- [4] Ohbuchi R, Masuda H, Aono M. Watermarking three-dimensional polygonal models. In *Proc. ACM International Conference on Multimedia'97*, Seattle, Nov. 9–13, 1997, pp.261–272.
- [5] Ohbuchi R, Masuda H, Aono M. Watermarking three-dimensional polygonal models through geometric and topological modifications. *IEEE J. Selected Areas in Communication*, 1998, 16(4): 551–560.
- [6] Ohbuchi R, Takahashi S, Miyazawa T et al. Watermarking 3D polygonal meshes in the mesh spectral domain. In *Proc. Graphics Interface*, Ottawa, Canada, June 7–9, 2001, pp.9–17.
- [7] Sun X, Rosin P L, Martin R R, Langbein F C. Fast and effective feature-preserving mesh denoising. *IEEE Trans. Visualization and Computer Graphics*, 2007, 13(5): 925–938.
- [8] Taubin G. A signal processing approach to fair surface design. In *Proc. SIGGRAPH'95*, Los Angeles, USA, August 6–11, pp.351–358.
- [9] Isenburg M, Gumhold S. Out-of-core compression for gigantic polygon meshes. In *Proc. SIGGRAPH'03*, San Diego, USA, July 27–31, pp.935–942.
- [10] Khodakovskiy A, Guskov I. Compression of Normal Mesh. Geometric Modeling for Scientific Visualization. Springer-Verlag, 2004, pp.189–206.
- [11] Peyre G, Mallat S. Surface compression with geometric bandlets. In *Proc. SIGGRAPH'05*, Los Angeles, USA, July 31–August 4, pp.601–608.
- [12] Rossignac J, Szymczak A. Wrap & zip decompression of the connectivity of triangle meshes compressed with edge breaker. *Computational Geometry, Theory and Applications*, 1999, 14(1/3): 119–135.
- [13] Watson B, Friedman A, McGaffey A. Measuring and predicting visual fidelity. In *Proc. SIGGRAPH'01*, Los Angeles, USA, August 12–17, pp.213–220.
- [14] Lindstrom P, Turk G. Image-driven simplification. *ACM Trans. Graph.*, 2000, 19(3): 204–241.
- [15] Corsini M, Gelasca E D, Ebrahimi T, Barni M. Watermarked 3-D mesh quality assessment. *IEEE Trans. Multimedia*, 2007, 9(2): 247–256.
- [16] Rogowitz B, Rushmeier H. Are image quality metrics adequate to evaluate the quality of geometric objects. In *Proc. SPIE Human Vis. Electron. Imag. VI*, Rogowitz B E, Pappas T N (eds.), Vol.4299, San Jose, USA, 2001, pp.340–348.
- [17] Aspert N, Santa-Cruz D, Ebrahimi T. Mesh: Measuring error between surfaces using the Hausdorff distance. In *Proc. IEEE Int. Conf. Multimedia and Expo*, Lusanne, Switzerland, August, 2002, pp.705–708.
- [18] Cignoni R S P, Rocchini C. Metro: Measuring error on simplified surfaces. *Comput. Graph. Forum*, 1998, 17(2): 167–174.
- [19] Williams N, Luebke D, Cohen J D, Kelley M et al. Perceptually guided simplification of lit, textured meshes. In *Proc. 2003 Symp. Interactive 3D Graphics*, Monterey, Canada, Feb. 27–March 1, A, 2003, pp.113–121.
- [20] Xun Z. Elasticity Mechanics. People's Education Press, 1979.
- [21] Wilhelm F. Tensor Analysis and Continuum Mechanics. Berlin: Springer-Verlag, 1972.
- [22] Chen W F, Salipu A F. Elasticity and Plasticity. China Architecture & Building Press, 2005.
- [23] Jones T R, Durand F, Desbrun M. Non-iterative, feature-preserving mesh smoothing. *ACM Trans. Graphics*, 2003, 21(3): 943–949.



Zhe Bian is a Ph.D. candidate at Department of Computer Science and Technology in Tsinghua University. His research interests include digital geometry processing. He is a student member of China Computer Federation.



Shi-Min Hu obtained his Ph.D. degree in 1996 from Zhejiang University. He is currently a chair professor of computer science at Tsinghua University. His research interests include digital geometry processing, video processing, rendering, computer animation, and computer-aided geometric design. He is on the editorial board of Computer Aided

Design, and he is a senior member of China Computer Federation.



Ralph R. Martin obtained his Ph.D. degree in 1983 from Cambridge University and is now professor at Cardiff University. He has published over 170 papers and 10 books covering such topics as solid and surface modeling, intelligent sketch input, geometric reasoning, reverse engineering, and various aspects of computer graphics. He is

on the editorial boards of Computer Aided Design and the International Journal of Shape Modelling.